Effects of composition on degree of order and ordering kinetics of Ni-Cr based superalloys

A. Marucco

JOURNAL DE PHYSIQUE IV
Colloque C7, supplément au Journal de Physique III, Volume 3, novembre 1993

Effects of composition on degree of order and ordering kinetics of Ni-Cr based superalloys

A. MARUCCO

CNR-ITM, Via Induno 10, 20092 Cinisello B., Milano, Italy

ABSTRACT

The ordering behaviour of different Ni–Cr base alloys, isothermally aged in the 450–600°C temperature range for up to 32000 h, was investigated by electrical resistivity measurements, lattice parameter determinations by X–ray diffraction and TEM observations. Degree of order and ordering kinetics were observed to depend on chemical composition, ageing time and temperature: SRO develops in all alloys during cooling from solution temperature and early stages of ageing with resistivity increments by up to 7% and lattice contractions by up to 0.05%. After 30000–32000 h ageing at temperatures below 500°C SRO transform to LRO in Brightray S, Nimonic 80A and Inconel 690 with sharp resistivity decreases of up to 16% and lattice contractions of up to 0.12%, whereas in the other alloys examined in this work only SRO structure was observed.

1. INTRODUCTION

An order transformation based on the formation of a Ni_2Cr phase has been widely observed in Ni–Cr base alloys aged below 600°C (1,2), resulting in lattice contraction due to the disordered *fcc* matrix changing to an ordered orthorhombic lattice. Atoms rearrangement causes deviations in physical properties: in particular, the electrical resistivity increases due to short–range order (SRO) but decreases sharply due to long–range order (LRO). Ordering is a nucleation and growth type process: the nucleation rate is higher at lower temperature but the growth rate, depending on atoms diffusion, increases with temperature. Hence, the degree of order depends on the thermal history of the sample but it also varies markedly depending on composition. SRO, well known to exist for Cr concentrations of 10–30%, has been recently detected in a Ni–Cr alloy with a Cr level as low as 1% (3), while LRO was detected in alloys with ~20% Cr aged below a critical temperature, T_c (1,2,4). LRO kinetics are relatively fast in stoichiometric Ni_2Cr alloy, but departing from this composition the transformation becomes very sluggish and requires several tens of thousands of hours to achieve completion. Furthermore, the degree of LRO mainly depends on Cr level but LRO kinetics is sensibly slowered by the addition of Fe. The effects of precipitation of other phases, such as γ', $Ni_3(Al,Ti)$ and α'–Cr, can overlap the ordering effects.

2. EXPERIMENTAL DETAILS

The chemical compositions of the alloys are reported in Tab. 1. Samples were subjected to a 2–stage standard solution treatment; the second stage of 16 h at 700°C was followed by water quench, in order to produce initially similar structures of the matrix in each alloy. Samples were isothermally aged in the 450–600°C range for up to 32000 h and then water quenched.
High precision d.c. resistance measurements were carried out at –196°C on each sample prior to any ageing and at interrupted annealing times with the conventional four–terminal potentiometric method. Lattice parameters were measured by X–ray diffraction. The microstructural evolution was observed by transmission electron microscopy techniques.

Table 1 – Chemical compositions of the alloys (wt%).

Alloy	Ni	Cr	Fe	Al	Ti	Others
Nimonic 75	72.35	19.40	4.28	0.13	0.36	(C 0.12,Co 0.4)
Nimonic 80A	75.32	19.50	0.81	1.41	2.40	(Co 2)
Nimonic 90	65.50	19.50	1.50	1.50	2.50	(Co 18)
Nimonic 105	49.35	14.85	1.00	4.70	1.30	(Co 20, Mo 5)
Nimonic 115	58.63	15.00	1.00	5.00	4.00	(Co 14, Mo 4)
Inconel 182	66.76	14.40	8.74	-	0.45	(Mn 7.2,Nb 1.8)
Inconel 690	60.46	29.20	8.85	0.26	0.26	
Inconel X-750	73.93	14.89	6.46	0.74	2.50	(Nb 0.93)
Sanicro 71	72.70	15.60	9.40	-	-	(Mn 0.79)
Brightray S	79.39	20.00	-	0.10	0.34	
T.D. NiCr	78.70	19.20	-	-	-	(ThO_2 2.01)
20Cr-25Ni steel	25.05	19.80	53.17	0.01	0.01	(Mn 0.8,Nb 0.6)

3. RESULTS AND DISCUSSION

Although the X-ray diffraction failed to provide any evidence for the ordered Ni_2Cr phase, due to the similarity of the atomic scattering factors of Ni and Cr, however, lattice parameter measurements indicate that all alloys contract on ageing below 550°C. Maximum contractions occur at 475°C (Tab.2). Extents of contractions differ, depending on the alloy composition, and can reach such an order of magnitude to generate dimensional instability and lead to excessive stresses in constrained components (4), can dominate any creep strain resulting in *negative creep* (5) and cause instantaneous strain bursts during creep (6). The presence of Mo in composition, giving rise to the formation of an ordered Ni_2Mo phase (7, 8), could account for large lattice contractions of Nimonic 105 and Nimonic 115.

Thin foil microstructural observations revealed *mottled contrast* and selected area diffraction patterns (SADP) are characterized by diffuse scattering. Both effects, previously attributed to SRO (9,10), appear after cooling from pre-treatment at 700°C and then are enhanced by ageing. The observation of Ni_2Cr superlattice spots in SADP of Nimonic 80A aged for 30000 h at 450°C (4) extended the Ni_2Cr phase field further than that considered by earlier authors (11). In this work *mottled contrast* was observed in Inconel 690 and Brightray S (Fig. 1 a,b) and, to a smaller extent, in Sanicro 71, 20Cr-25Ni steel, Nimonic 75 and TD NiCr but the homogeneous precipitation of fine γ' masked this effect in Inconel X-750. Dislocation pile-ups in absence of evident obstacles, typical of SRO structures, were frequently observed.

Ni_2Cr superlattice spots were not observed neither in Inconel 690 with a very high Cr level nor in Brightray S with a Cr level similar to Nimonic 80A. In spite of that, both alloys are supposed to be susceptible to form LRO on prolonged ageing, since kinetics are retarded in the former alloy by the presence of 9% Fe in composition while in the latter alloy by a higher Ni content, as compared to Nimonic 80A, and by the absence of the γ' phase, which enhances the LRO formation in Nimonic 80A (12). This is supported by the observation of few ordered domains in the microstructure of Inconel 690 and by resistivity drop in Brightray S after 30000 h at $T \leq 500$°C (Fig. 2).

The isothermal resistivity curves of different alloys are characterized by increments of up to 7% during the first hours followed by a plateau. Resistivity rise is due to electrons scattering by SRO nuclei(13). Maximum is function of temperature corresponding to a particle size comparable with the wave length of electrons at the Fermi level (14). The plateau at maximum value suggests a stable precipitate size satisfying the Aubauer's criteria for non-coarsening structures (15). The equilibrium values are correlable to SRO degree of the alloy at each temperature. SRO kinetics show only little dependence on composition and temperature, if any, but SRO degree sensibly decreases with temperature and does not disappear suddenly when T_c is exceeded but vanishes gradually. The SRO degree decreases with increasing Fe level in Ni-Cr-Fe alloys but low degrees of SRO were also detected in Fe-rich alloys (2) and in 20Cr-25Ni steel. Moreover, comparing the equilibrium values of alloys with similar Fe levels it appears that SRO degree increases linearly with Ni concentration (Fig. 3). The higher rise observed in Ni-rich alloys lead early authors to assume simply the formation of an ordered phase with Ni_3Cr composition (16), but X-ray diffraction showed that lattice parameter decreases with increasing Ni level (17), hence the larger effect of SRO on resistivity of Ni-rich alloys is supposed to depend on the increase of the electron scattering factor by Ni_2Cr nuclei with decreasing the atomic density of the alloy.

Table 2 – Lattice contractions upon ageing at 475°C (%).

Alloy	1000 h	10 000 h	20 000 h	32 000 h
Nimonic 80A	0.024	0.035	0.107	0.120
Nimonic 90	0.027	0.034	0.074	-
Nimonic 105	0.045	0.067	0.089	-
Nimonic 115	0.065	0.079	0.102	-
Inconel 690	0.020	0.038	0.038	0.049
Inconel X-750	0.015	0.022	0.038	-
Sanicro 71	0.005	0.022	0.032	0.035
20Cr-25Ni steel	0.014	0.024	0.020	0.033

Sudden resistivity drops in Brigthray S and Nimonic 80A (Fig. 2b) long-term aged below 500°C are due to the coalescence and growth beyond the critical size of ordered zones, i.e. to the SRO to LRO transition. An otherwise unexplained resistivity change can not be ascribed to LRO but other phase transformations must be considered. Gradual resistivity decreases in Inconel 690 and Brightray S at 550-600°C are determined by the α'-Cr precipitation. Amount and size of those precipitates, usually at grain boundaries, increase with time and temperature of ageing as well as the magnitude of resistivity decrement, which is due to Cr depletion of the matrix (18), but lattice parameter value is not affected (19). The effects of the homogeneous γ' precipitation overlap those of SRO, since both phases nucleate in the mean time and lead to resistivity increment but γ' particles ripens at a faster rate and, as soon as the critical size is exceeded, they cause reductions larger than the SRO-induced increments, as observed in Inconel X-750 (20). The γ' precipitation also accounts for larger resistivity increments in Nimonic 80A as compared to Brightray S. Finally, sharp resistivity increase after prolonged ageing of 20Cr-25Ni steel at 600 and, to a smaller extent, at 550°C is possibly due to σ precipitation (Fig.2d).

ACKNOWLEDGEMENTS

The author is indebted to Dr. B. Nath for providing aged alloys and many helpful discussions and to Mr. G. Carcano and Mr. E. Signorelli for valuable assistance with the experimental work.

REFERENCES

[1] MARUCCO A. and NATH B., J. Mat. Sci. **23** (1988) 2107.
[2] MARUCCO A., Key Engng. Mat. **48** (1990) 77.
[3] MUTH P. and HEIMKE W., Phys. Stat. Sol.(a) **126** (1991) K69.
[4] METCALFE E., NATH B. and WICKENS A., Mat. Sci. Engng **67** (1984) 157.
[5] FOUNTAIN R.W. and KIRCHYNSKY M., Trans ASM **51** (1959) 108.
[6] KLUEH R.L., Mat. Sci. Engng. **54-1** (1982) 65.
[7] TAWANCY H.M., J. Mat. Sci. **16** (1981) 2883.
[8] SRIVASTAVA S.K. and ROTHMAN M.F., Proc. Int. Conf. on High Temperature Materials for Power Engineering, E. Bachelet et al.(Ed.s), Kluwer Academic Publishers (1990) 1357.
[9] BAGARIATSKII Yu.A. and TIAPKIN Yu.D., Sov. Phys. Dok., **3** (1958) 1025.
[10] HIRABAYASHI M. et al., Trans Japan Inst. Met. **10** (1969) 365.
[11] VINTAYKIN Y.Z. and URUSHADZE G.G., Fiz. Met. Metall. **27** (1969) 895.
[12] MARUCCO A. and NATH B., Proc. Int. Conf. on High Temperature Materials for Power Engineering, E.Bachelet et al.(Ed.s), Kluwer Academic Publishers (1990) 535.
[13] THOMAS H., Z. Physik **129** (1951) 219.
[14] MOTT N.F., J. Inst. Met. **50-1** (1937) 267.
[15] AUBAUER H.P., Phys. Stat. Sol.(a) **43** (1977) 261 and 601.
[16] TAYLOR A. and HINTON K.G., J. Inst. Metals **81** (1952) 169.
[17] MARUCCO A., Mat. Sci. Forum, Trans. Tech. Publ. **79-82** (1991) 575.
[18] GROBNER P.J., Met. Trans. **4** (1973) 251.
[19] MARUCCO A. and SIGNORELLI E., Proc. Int. Conf. on Intergranular and Interphase Boundaries in Materials '92, Thessaloniki, Greece, Trans. Tech. Publ., in press.
[20] LANG E., LUPINC V. and MARUCCO A., Mat. Sci. Engng. **A114** (1989) 157.

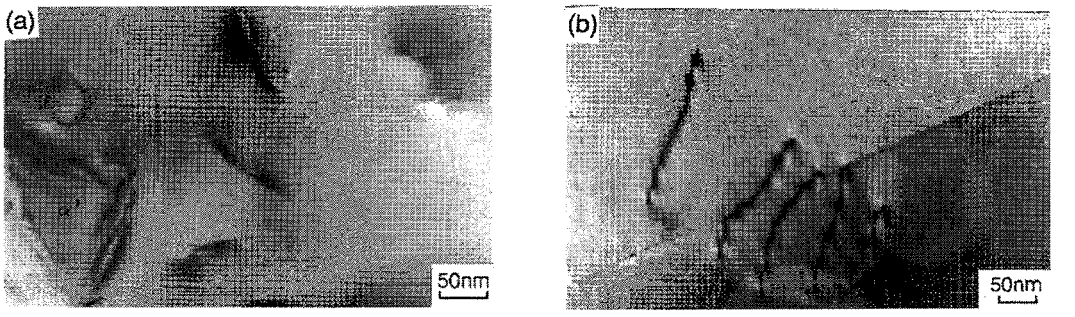

Fig.1 Microstructures of (a) Inconel 690, 475°C, 32000 h and (b) Brightray S, 500°C, 30000 h.

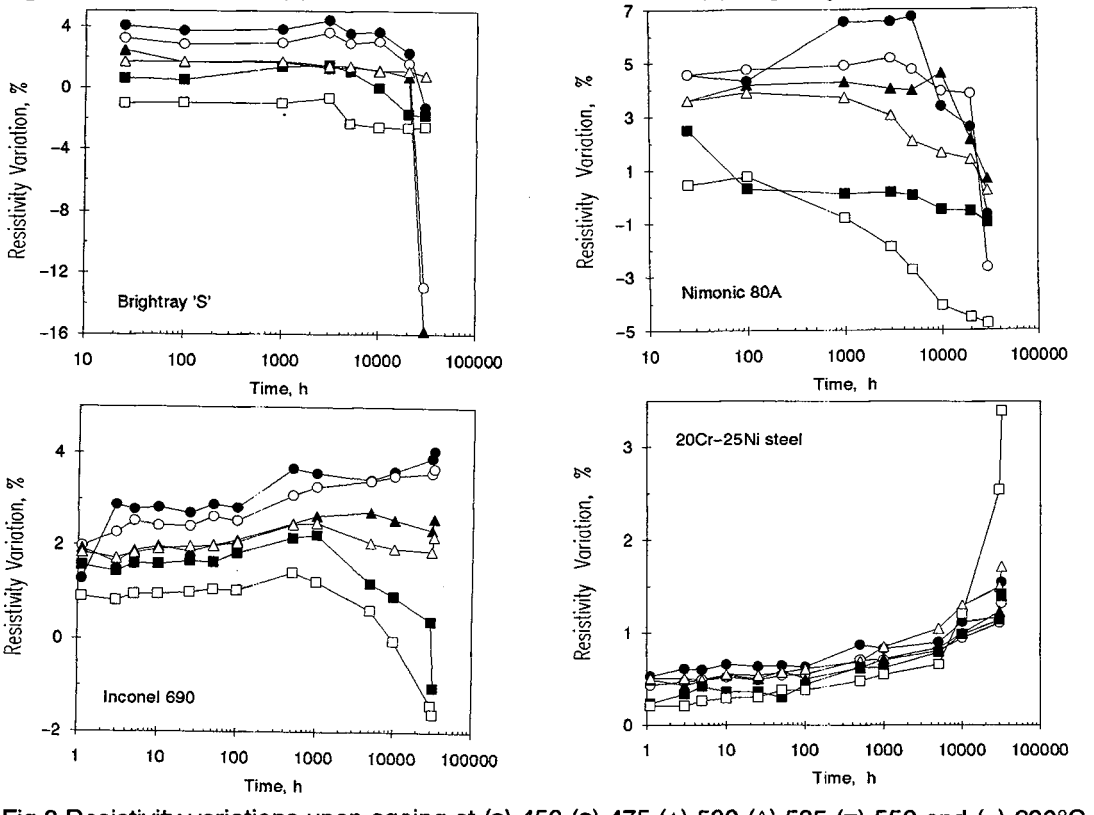

Fig.2 Resistivity variations upon ageing at (●) 450,(○) 475,(▲) 500,(△) 525,(■) 550 and (□) 600°C.

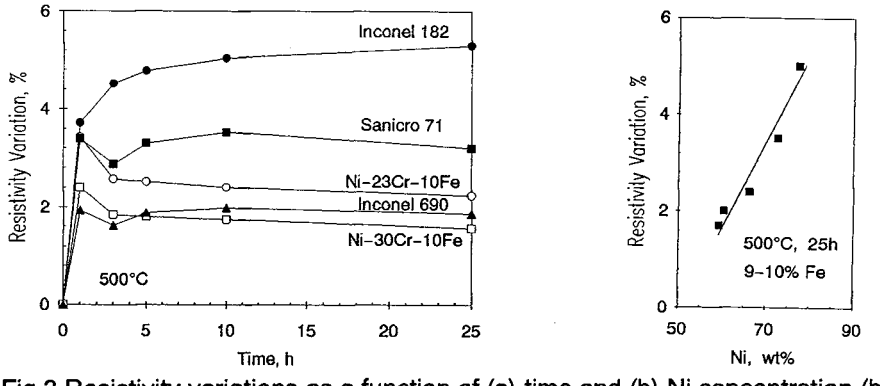

Fig.3 Resistivity variations as a function of (a) time and (b) Ni concentration (b).